



<http://www.diva-portal.org>

## Postprint

This is the accepted version of a paper published in *Nuclear Medicine and Biology*. This paper has been peer-reviewed but does not include the final publisher proof-corrections or journal pagination.

Citation for the original published paper (version of record):

Honarvar, H., Jokilaakso, N., Andersson, K., Malmberg, J., Rosik, D. et al. (2013)  
Evaluation of backbone-cyclized HER2-binding 2-helix Affibody molecule for In Vivo  
molecular imaging.  
*Nuclear Medicine and Biology*, 40(3): 378-386  
<http://dx.doi.org/10.1016/j.nucmedbio.2012.12.009>

Access to the published version may require subscription.

N.B. When citing this work, cite the original published paper.

Permanent link to this version:

<http://urn.kb.se/resolve?urn=urn:nbn:se:uu:diva-198614>

**NOTICE:** this is the author's version of a work that was accepted for publication in Nuclear Medicine and Biology. Changes resulting from the publishing process, such as editing, corrections, structural formatting, and other quality control mechanisms may not be reflected in this document. Changes may have been made to this work since it was submitted for publication.

A definitive version was subsequently published in:

Honarvar H, Jokilaasko N, Andersson K, Malmberg J, Rosik D, Orlova A, Eriksson Karlström A, Tolmachev V, Järver P. Evaluation of Backbone-Cyclized HER2-Binding Two-Helix Affibody Molecule for In Vivo Molecular Imaging. *Nucl Med Biol*, 2013;40(3):378-86. DOI 10.1016/j.nucmedbio.2012.12.009.

<http://www.sciencedirect.com/science/article/pii/S0969805112003204>

### **Evaluation of Backbone-Cyclized HER2-Binding 2-Helix Affibody Molecule for *In Vivo* Molecular Imaging**

Hadis Honarvar,<sup>a</sup> Nima Jokilaakso,<sup>b</sup> Karl Andersson,<sup>a,c</sup> Jennie Malmberg,<sup>d</sup> Daniel Rosik,<sup>b</sup> Anna Orlova,<sup>d</sup> Amelie Eriksson Karlström,<sup>b</sup> Vladimir Tolmachev<sup>a\*</sup> & Peter Järver<sup>b,e</sup>

<sup>a</sup> Unit of Biomedical Radiation Sciences, Rudbeck Laboratory, Uppsala University, Sweden;

<sup>b</sup> Division of Molecular Biotechnology, School of Biotechnology, KTH Royal Institute of Technology, AlbaNova University Centre, Stockholm, Sweden;

<sup>c</sup> Ridgeview Instruments AB, Uppsala, Sweden;

<sup>d</sup> Preclinical PET Platform, Department of Medicinal Chemistry, Uppsala University, Uppsala, Sweden;

<sup>e</sup> Present address: MRC Laboratory of Molecular Biology, PNAC Division, Cambridge, UK

\* Corresponding author:

Vladimir Tolmachev  
Biomedical Radiation Sciences  
Rudbeck Laboratory  
Uppsala University  
S-751 81 Uppsala  
Sweden  
Phone: +46 18 471 3414  
Fax: + 46 18 471 3432  
[Vladimir.tolmachev@bms.uu.se](mailto:Vladimir.tolmachev@bms.uu.se)

## ABSTRACT

**Introduction.** Affibody molecules, small scaffold proteins, have demonstrated an appreciable potential as imaging probes. Affibody molecules are composed of three alpha-helices. Helices 1 and 2 are involved in molecular recognition, while helix 3 provides stability. The size of Affibody molecules can be reduced by omitting the third alpha-helix and cross-linking the two remaining, providing a smaller molecule with better extravasation and quicker clearance of unbound tracer. The goal of this study was to develop a novel 2-helix Affibody molecule based on backbone cyclization by native chemical ligation (NCL).

**Methods.** The HER2-targeting NCL-cyclized Affibody molecule  $Z_{\text{HER2}:342\text{min}}$  has been designed, synthesized and site-specifically conjugated with a DOTA chelator. DOTA- $Z_{\text{HER2}:342\text{min}}$  was labeled with  $^{111}\text{In}$  and  $^{68}\text{Ga}$ . The binding affinity of DOTA- $Z_{\text{HER2}:342\text{min}}$  was evaluated *in vitro*. The targeting properties of  $^{111}\text{In}$ - and  $^{68}\text{Ga}$ -DOTA- $Z_{\text{HER2}:342\text{min}}$  were evaluated in mice bearing SKOV-3 xenografts and compared with the properties of  $^{111}\text{In}$ - and  $^{68}\text{Ga}$ -labeled PEP09239, a DOTA-conjugated 2-helix Affibody analogue cyclized by a homocysteine disulfide bridge.

**Results.** The dissociation constant ( $K_D$ ) for DOTA- $Z_{\text{HER2}:342\text{min}}$  binding to HER2 was 18 nM according to SPR measurements. DOTA- $Z_{\text{HER2}:342\text{min}}$  was labeled with  $^{111}\text{In}$  and  $^{68}\text{Ga}$ . Both conjugates demonstrated bi-phasic binding kinetics to HER2-expressing cells, with  $K_{D1}$  in low nanomolar range. Both variants demonstrated specific uptake in HER2-expressing xenografts. Tumor-to-blood ratios at 2 h p.i. were  $6.1 \pm 1.3$  for  $^{111}\text{In}$ -DOTA- $Z_{\text{HER2}:342\text{min}}$  and  $4.6 \pm 0.7$  for  $^{68}\text{Ga}$ -DOTA- $Z_{\text{HER2}:342\text{min}}$ . However, the uptake of DOTA- $Z_{\text{HER2}:342\text{min}}$  in lung, liver and spleen was appreciably higher than the uptake of PEP09239-based counterparts.

**Conclusions.** Native chemical ligation enables production of a backbone-cyclized HER2-binding 2-helix Affibody molecule ( $Z_{\text{HER2}:342\text{min}}$ ) with low nanomolar target affinity and specific tumor uptake.

Key words: Affibody; HER2; 2-helix protein; SPPS; native chemical ligation, biodistribution

## INTRODUCTION

Affibody molecules are a class of small (7 kDa) scaffold proteins, which are composed of a 3-helix cysteine-free bundle consisting of 58 amino acids [1]. Affibody molecules can be selected to bind different proteins with high affinity by randomization of thirteen amino acids on helices 1 and 2 [2]. Their small size facilitates high rates of extravasation and tissue penetration, and rapid blood clearance of unbound tracer molecules [3]. High-affinity Affibody molecules have been selected for binding to cancer-associated molecular targets such as HER2 (human epidermal growth factor receptor type 2) [4], EGFR (epidermal growth factor receptor) [5], HER3 (human epidermal growth factor receptor type 3) [6], PDGFR $\beta$  (platelet derived growth factor receptor  $\beta$ ) [7] and IGF1R (insulin-like growth factor 1 receptor) [8]. Preclinical studies, including direct comparison experiments, have demonstrated that Affibody molecules provide higher imaging contrast than radiolabeled antibodies [9, 10], and clinical studies have confirmed high potential for Affibody molecules in molecular imaging [11,12]

The binding surface of Affibody molecules localizes only on helices 1 and 2, while helix 3 provides stability to the structure. In principle, helix 3 might be removed if the scaffold rigidity could be provided by other means [13]. In order to develop a 2-helix Affibody molecule targeting HER2, the previously described Affibody molecules named Z<sub>HER2:342</sub>, and a 2-helix version of the IgG-binding Z domain, denoted Z34C, were used as design templates [4, 13]. Webster and co-workers [14] have shown that introduction of a disulfide bridge between the C-and N-termini stabilizes the 2-helix structure and permits peptide synthesis of 2-helix Affibody molecules with retained binding specificity to HER2, although at a cost of substantial reduction of affinity (3 orders of magnitude). Further optimization of the sequence

and the use of homocysteine for disulfide bridge formation allowed obtaining a 2-helix Affibody variant with affinity of 5 nM [14]. Although this affinity is appreciably lower than the affinity of parental Affibody molecules  $Z_{\text{HER2:342}}$  (22 pM, [4]), it is still sufficient for imaging applications [15]. A DOTA-conjugated 2-helix variant, DOTA-MUT-DS (other designation PEP09239), has previously been labeled with  $^{68}\text{Ga}$ ,  $^{64}\text{Cu}$  and  $^{111}\text{In}$ , and successfully used for imaging of HER2-expressing tumor xenografts in mice [16-18]. Direct *in vivo* comparison of the biodistribution properties of  $^{111}\text{In}$ -PEP09239 and its parental 3-helix Affibody molecule  $^{111}\text{In}$ -ABY-002 [4] showed that although the absolute tumor uptake values were higher for the 3-helix variant, the 2-helix variant showed higher tumor-to-blood ratio [18]. The results of these studies suggest that novel and robust disulfide-stabilized 2-helix scaffolds are promising molecular probes for imaging applications. However, these variants have unprotected termini, which make them potentially sensitive to exoproteases. Furthermore, the disulfide bond in their structure restricts selection of labeling methods. The use of methods requiring the use of strong reducing agents (e.g. labeling with  $^{99\text{m}}\text{Tc}$ ) might be complicated.

Recently, we have developed an alternative approach to stabilization of 2-helix Affibody molecules based on backbone cyclization by native chemical ligation (NCL) [19]. This approach was applied to the parental IgG-binding Affibody molecule (the Z-domain) resulting in a new format denoted  $Z_{\text{min}}$ . In this study, the loss of affinity in comparison with its 3-helix parental variant was modest, from  $K_{\text{D}} = 3$  to 15 nM. The backbone cyclization by NCL leaves a cysteine residue at the ligation point between helices 1 and 2, and this residue might be used as a chemo-selective handle for conjugation of chelators and linkers for radionuclides. This strategy eliminates the risk of thiol-disulfide exchange or reduction of the disulfide.

Other advantageous properties of a smaller 2-helix scaffold, such as possible higher tissue penetration, are preserved in this design.

In the current study, we applied NCL for development of a 2-helix anti-HER2 Affibody molecule. When removing the stabilizing third helix from the Affibody scaffold, the hydrophobic core of the scaffold is exposed to the environment and specific mutations must be introduced in helices 1 and 2 in order to retain protein solubility. Braisted *et al.* performed a thorough step-wise selection of random mutations to produce a soluble, high-affinity 2-helix version of the Z-domain [20]. We applied the described substitutions, in combination with substitutions introduced to facilitate synthesis of a backbone-cyclized version of the Z-domain to the HER2-binding Z<sub>HER2:342</sub> Affibody molecules (for sequence, see **Figure 1D**). The resulting 2-helix Affibody molecule is a combination between the previously published sequences of Z34C [20] and Z<sub>HER2:342</sub> [11] and was designated Z<sub>HER2:342min</sub>. The Z<sub>HER2:342min</sub> molecule was evaluated in terms of affinity, selectivity and thermal stability. After site-specific conjugation with maleimido-DOTA, the Z<sub>HER2:342min</sub> was labeled with radionuclides <sup>111</sup>In and <sup>68</sup>Ga. Binding of <sup>111</sup>In- and <sup>68</sup>Ga- DOTA-Z<sub>HER2:342min</sub> to living HER2-expressing cells and their biodistribution and tumor targeting properties were evaluated and compared with the properties of <sup>111</sup>In- and <sup>68</sup>Ga-PEP09239.

## MATERIAL AND METHODS

### Material

Z<sub>HER2:342min</sub> was assembled by the following Fmoc-protected amino acids with respective side-chain protecting groups: *tert*-butyloxycarbonyl (Boc) for Lys and Trp, *tert*-butyl (tBu) for Ser, Thr and Tyr, *tert*-butyl ester (OtBu) for Asp and Glu, trityl (Trt) for Gln, Cys, Asn and His and pentamethyldihydrobenzofuran-5-sulfonyl (Pbf) for Arg. Cys was Boc-protected, with Trt side-chain protecting group. The Dawson Dbz AM resin (3-(Fmoc-amino)-4-aminobenzoyl AM resin (100-200 mesh), loading 0.43 mmol/g, was from Novabiochem. The activating reagents used were 1-hydroxybenzotriazole monohydrate (HOBt\*H<sub>2</sub>O) and 2-(1H-benzotriazol-1-yl)-1,1,3,3-tetramethyluronium hexafluorophosphate (HBTU) from Iris Biotech GmbH, Germany. Maleimido-monoamide-DOTA was obtained from Macrocylics, Dallas, TX. Recombinant Fc fusions of the extracellular domains of human HER2 (ErbB2) and HER3 (ErbB3) were from R&D Systems, MN, USA.

Buffers, such as 0.1 M phosphate-buffered saline (PBS), pH 7.5, and 0.2 M ammonium acetate, pH 5.5, and 1.25 M sodium acetate, pH 3.6, were prepared using high-quality Milli-Q water (resistance higher than 18 M $\cdot$ cm). Metal contamination was removed from the buffers used for labeling by purification using 2–3 g/l Chelex 100 resin (Bio Rad Laboratories, Richmond, CA, USA). PEP09239 was produced as described earlier [18]. [<sup>111</sup>In]Indium chloride was purchased from Covidien. The <sup>68</sup>Ge/<sup>68</sup>Ga generator (Eckert and Ziegler AG, Germany) was eluted with 0.1 M hydrochloric acid (prepared from 30% ultra-pure HCl from Merck).

The human ovarian carcinoma cell line SKOV3 (ATCC, purchased via LGC Promochem, Borås, Sweden) was used in the experiments. The cell lines for LigandTracer test and for tumor implantation study were cultured in RPMI medium (Flow Irvine, UK) supplemented with 10 % fetal calf serum (Sigma, USA), 2 mM L-glutamine and PEST (penicillin 100 IU/mL and 100 µg/mL streptomycin), all from Biokrom Kg, Germany. Ketamine (50 mg/ml, Ketalar; Pfizer, New York, NY), xylazine (20 mg/ml, Rompun; Bayer, Leverkusen, Germany), and heparin (5,000 IE/ml; Leo Pharma, Copenhagen, Denmark) were obtained commercially.

The yield of the labeled Affibody constructs was determined using 150–771 DARK GREEN, Tec-Control Chromatography strips from Biodex Medical Systems (Shirley, NY, USA), eluted with 0.2 M citric acid, pH 2.0. Sodium dodecyl sulfate polyacrylamide gel electrophoresis (SDS-PAGE), 200 V constant, was performed using NuPAGE 4–12% Bis-Tris Gel (Invitrogen AB, Lidingö, Sweden) in MES buffer (Invitrogen AB, Lidingö, Sweden) to confirm the identity of  $^{68}\text{Ga}$ -DOTA-Z<sub>HER2:342min</sub>. The distribution of radioactivity along the thin layer chromatography strips and electrophoresis gels was measured on a Cyclone storage phosphor system and analyzed using OptiQuant image analysis software. The radioactivity was measured using an automated gamma-counter with a 3-inch NaI (Tl) detector (1480 Wizard; Wallac Oy, Turku, Finland).

Data on cellular uptake and biodistribution were analyzed by two-tailed t-test using GraphPad Prism (version 4.00 for Windows; GraphPad Software, San Diego, CA) in order to determine the significance of differences ( $p < 0.05$ ).

## General Procedure of Z<sub>HER2:342min</sub> Synthesis

Assembly of Z<sub>HER2:342min</sub> was carried out on a Dbz-functionalized amide resin. The peptide sequence CGFSKEMRNRYWEAALDPNLTNQQKRAKIRSIYEEG was assembled in a step-wise manner on a 433A Peptide Synthesizer (Applied Biosystems) using Fmoc/tBu strategy. The syntheses were carried out in 0.1 mmol scale and all amino acids were coupled in 10-fold excess. The protocol was based on a standard protocol from the SynthAssist® 2.0 software (chemistry: FastMoc0.1 MonPrevPeak, Applied Biosystems). Fmoc deprotection was monitored in real-time by conductivity measurements. HOBt/HBTU (10 eq.) in the presence of DIEA (15 eq.) was used to activate the -carboxyl group prior to coupling. In order to avoid acetylation of the Dbz linker, conventional Ac<sub>2</sub>O capping of the uncoupled free amines was not performed. After completed synthesis, Dbz was converted to *N*-acyl-benzimidazolinone (Nbz) in order to form a C-terminal ester as performed earlier [19]. Briefly, 4-nitrophenylchloroformate (5 eq.) in DCM was added (40 min) to the peptide-resin for specific acylation, followed by deprotonation and cyclization of the linker with 0.5 M DIEA in DCM [28].

Cleavage from the solid support was performed using a standard Fmoc protocol. Briefly, the peptide-resin was treated for 2 h at room temperature with a cleavage solution consisting of TFA/EDT/H<sub>2</sub>O/TIS (94:2.5:2.5:1). Cleavage from the solid phase was followed by three rounds of extraction with *tert*-butyl methyl ether and H<sub>2</sub>O (3:1), and the aqueous phase was then filtered, frozen, and lyophilized.

## Purification and Analysis of Z<sub>HER2:342min</sub>

The linear peptide was purified and analyzed by Reversed Phase High Performance Liquid Chromatography (RP-HPLC) (Agilent Technologies) with an elution gradient of 35-55% acetonitrile-0.1% TFA for 20 min at a flow rate of 2.5 ml/min on a 10 mm×250 mm C18 column with 5 μm particle size (semi preparative, Reprosil Gold 300, Dalco Chromtech AB). The collected fractions were frozen and lyophilized. The theoretical molecular weight of the peptide was calculated from its molecular formula C<sub>186</sub>H<sub>291</sub>N<sub>57</sub>O<sub>56</sub>S<sub>2</sub>. The peptide mass was confirmed by ESI-MS (6520 Accurate Mass Q-TOF LC/MS, Agilent Technologies), coupled to RP-HPLC using a 300 μm×5 mm C4 column, particle size 5 μm (Acclaim PepMap300, LC Packings - Genetech). The concentration of the peptide was determined by absorbance measurements using Eppendorf BioPhotometer (Eppendorf) and the concentration was calculated using Beer-Lambert's law (extinction coefficient=8480 M<sup>-1</sup>cm<sup>-1</sup>).

### **Cyclization and Purification of Z<sub>HER2:342min</sub>**

Backbone cyclization of the peptide was carried out over 2 h using the ligation buffer Na<sub>2</sub>HPO<sub>4</sub>/MPAA/TCEP (0.2 M: 0.2 M: 0.02 M), pH 7. Purification of the cyclized product was performed by semi-preparative RP-HPLC using a gradient of 35-55% acetonitrile-0.1% TFA, at a flow rate of 2.5 ml/min with the same column and solvent system as described above for the linear peptide. Up to three repetitive rounds of RP-HPLC purification were required in order to remove all the excess of MPAA from the cyclization step.

### **DOTA Conjugation**

5 equivalents of maleimido-DOTA (Macrocyclics) were coupled to the free Z<sub>HER2:342min</sub> cysteine residue in a 5 mM NaOAc buffer, pH 5.5, for 2 h at room temperature. DOTA-Z<sub>HER2:342min</sub> (PEP12718) was then purified by RP-HPLC and the conjugation was confirmed by ESI-MS as described above.

### **Circular Dichroism Analysis**

The helicity of DOTA-Z<sub>HER2:342min</sub> was investigated by Circular Dichroism (CD). The CD spectra were collected using a Jasco J-810 spectropolarimeter (Jasco Scandinavia AB), and recorded in 0.1 nm intervals over a 190-250 nm spectra in a 0.1 cm quartz cell at 20°C. Peptide concentration was 0.5 mg/ml. The melting temperature was determined over a heat gradient (20-90°C) at 220 nm. To study refolding of DOTA-Z<sub>HER2:342min</sub>, the helical content was measured for a second time after heat treatment. All CD spectra represent an average of three assembled scans.

### **Surface Plasmon Resonance Analysis of Binding Kinetics**

Surface Plasmon Resonance (SPR) analysis of the DOTA-Z<sub>HER2:342min</sub> binding to a chimeric protein composed of the extracellular domain of human HER2 or HER3 fused to an antibody Fc-region (HER2-Fc and HER3-Fc, R&D Systems) was performed on a Biacore 2000 instrument (GE Healthcare). Dextran-coated CM5 sensor chips were activated by EDC/NHS, followed by immobilization of HER2-Fc at a concentration of 10 µg/ml in 10 mM NaOAc buffer, pH 4.5. The protein immobilization resulted in a response of approximately 3,500 response units (RU) for HER2-Fc and about 1,000 RU for the negative control, HER3-Fc. Interaction analysis was performed at 25°C in HBS-EP buffer (10 mM HEPES, 150 mM

NaCl, 3.4 mM EDTA, 0.005% Tween 20, pH 7.4) with a flow rate of 25  $\mu$ l/min. 30  $\mu$ l samples with concentrations ranging from 2.1 to 67 nM were injected over the immobilized receptor and regeneration of the surfaces between each injection was carried out with 20  $\mu$ l injections of 15 mM HCl. All calculations were performed in the BiaEval software (GE Healthcare) and the  $K_D$  constant for DOTA-Z<sub>HER2:342min</sub> binding to HER2-Fc was determined with a  $\chi^2$  value below 1.

### **Radiolabeling of Conjugates with <sup>111</sup>In and <sup>68</sup>Ga**

For labeling with <sup>111</sup>In, a lyophilized DOTA-Z<sub>HER2:342min</sub> was reconstituted in 0.2 M ammonium acetate, pH 5.5, at 1 mg/ml concentration. Aliquots containing 38.4  $\mu$ g of the conjugate were stored and frozen at -20°C. Immediately before labeling, an aliquot of a conjugate was mixed with predetermined amounts of <sup>111</sup>In-chloride solution (ca. 30 MBq at calibration time). The reaction mixtures were incubated at 90°C for 30 min. Thereafter, a small aliquot (1  $\mu$ l) of reaction mixture was taken and analyzed by radio-ITLC eluted with 0.2 M citric acid, pH 2.0. In this system, radiolabelled proteins remain at the application point while free <sup>111</sup>In migrates with the solvent front. PEP09239 was labeled with <sup>111</sup>In for comparative biodistribution and kinetic interaction experiments as described previously [18].

For labeling with <sup>68</sup>Ga, the generator was eluted with 0.1 M HCl, and two fractions of eluate, 900  $\mu$ l (void volume) and 700  $\mu$ l, were collected. The second fraction (700  $\mu$ l) containing the maximum radioactivity was used for labeling. A freeze-dried aliquot of DOTA-Z<sub>HER2:342min</sub> (38.4  $\mu$ g) was mixed with 80 or 40 MBq <sup>68</sup>Ga-containing eluate and incubated at 95°C for 15 min. Thereafter, small aliquots (1  $\mu$ l) of reaction mixtures were taken and analyzed by radio-ITLC eluted with 0.2 M citric acid, pH 2.0. In this system, radiolabelled proteins remain at the

application point while free  $^{68}\text{Ga}$  migrates with the solvent front. Identity of the radioconjugate was cross-validated using SDS-PAGE. PEP09239 was labeled with  $^{68}\text{Ga}$  for comparative biodistribution and kinetic interaction experiments in the same way as DOTA- $Z_{\text{HER2}:342\text{min}}$ .

The stability of  $^{111}\text{In}$ -DOTA- $Z_{\text{HER2}:342\text{min}}$  and  $^{68}\text{Ga}$ -DOTA- $Z_{\text{HER2}:342\text{min}}$  was evaluated by challenge with 500-fold excess of EDTA during 1 h as described earlier [21].

### **Measurements of Affinity of 2-Helix Affibody Molecules Binding to Living HER2-Expressing Cells using LigandTracer Yellow**

Cells from the human ovarian carcinoma cell line SKOV-3 were seeded on a local area of a cell culture dish (Nunclon<sup>TM</sup>, Size 100620, NUNC A/S, Roskilde, Denmark), as described previously [22]. The binding of  $^{111}\text{In}$ -DOTA- $Z_{\text{HER2}:342\text{min}}$  and  $^{68}\text{Ga}$ -DOTA- $Z_{\text{HER2}:342\text{min}}$  to living cells was monitored in real-time at room temperature using LigandTracer Yellow, using established methods [22]. In brief, the cell culture dish was placed on the sloping and rotating cell dish holder in LigandTracer Yellow, followed by a continuous monitoring of the radioactivity level along the rim of the dish. If the labeled Affibody molecule binds to the cells, an elevated signal will be recorded when the cells pass by the detector. This makes it possible to accurately detect binding events both during incubation and after wash [22]. In order to cover the concentration span needed for proper affinity estimation entirely, two increasing concentrations (selected based on the Biacore results: 30 nM and 100 nM which corresponds to approximately the  $K_D$  value and 3-4 times the  $K_D$  value) of  $^{111}\text{In}$ -DOTA- $Z_{\text{HER2}:342\text{min}}$  and  $^{68}\text{Ga}$ -DOTA- $Z_{\text{HER2}:342\text{min}}$  were added in each affinity titration assay. Each concentration was incubated long enough to approach steady state. Thereafter, the ligand

solution was replaced with fresh medium and the dissociation rate was followed overnight ( $^{111}\text{In}$ -labeled compound) or a few hours ( $^{68}\text{Ga}$ -labeled compound). The equilibrium dissociation constant  $K_D$  of  $^{68}\text{Ga}$ -DOTA- $Z_{\text{HER2}:342\text{min}}$  and  $^{111}\text{In}$ -DOTA- $Z_{\text{HER2}:342\text{min}}$  interaction was estimated using data from the stepwise titration affinity experiments. The signal levels from the end of each incubation assay, representing approximately steady-state, were analyzed using a non-linear regression model describing a 1:2 interaction. The data were decay corrected for both  $^{111}\text{In}$  and  $^{68}\text{Ga}$  (including  $^{68}\text{Ge}$  breakthrough).

Binding interaction of  $^{111}\text{In}$ -PEP09239 and  $^{68}\text{Ga}$ -PEP09239 were evaluated under the same condition, with the exception that different concentrations were used (6.3 and 18.9 nM).

### **Comparative *In Vivo* Studies**

The goal of the study was a comparative evaluation of  $^{68}\text{Ga}$  and  $^{111}\text{In}$  influence on the biodistribution and targeting properties of DOTA- $Z_{\text{HER2}:342\text{min}}$ . All animal experiments were planned and performed in accordance with the national regulation on laboratory animals' protection and were approved by the local Ethics Committee for Animal Research in Uppsala. In order to reduce the number of animals in the experiments, a dual-label approach was used when both  $^{68}\text{Ga}$ - and  $^{111}\text{In}$ -labelled tracers were co-injected in the same mice.

Comparison of tumor targeting was performed in BALB/c *nu/nu* mice (weight  $21.3 \pm 0.9$  g) bearing SKOV-3 xenografts. Cells ( $10^7$  cells per mouse) were implanted subcutaneously on the right hind leg 5 weeks before the experiment. At the time of experiment, the average tumor weight was  $92.08 \pm 0.03$  mg. The mice were injected intravenously (tail vein) with a mixture of 10 kBq  $^{111}\text{In}$ -DOTA- $Z_{\text{HER2}:342\text{min}}$  and 380 kBq of  $^{68}\text{Ga}$ -DOTA- $Z_{\text{HER2}:342\text{min}}$  in 100  $\mu\text{l}$  PBS. The total injected peptide dose was adjusted to 3.72  $\mu\text{g}$  per animal by non-labeled

Z<sub>HER2:342min</sub>. The standards of injected radioactivity as well as a standard of <sup>111</sup>In were prepared at the time of injection. To check the specificity of xenograft targeting, a group of four mice was subcutaneously pre-injected with 500 µg (3800 nmol) non-labeled recombinant Z<sub>HER2:342min</sub> Affibody molecule. The mice were euthanized at predetermined time points (1 and 2 h p.i.) by an intra-peritoneal injection of Ketalar-Rompun solution (20 µl of solution/g body weight: Ketalar, 10 mg/ml; Rompun, 1 mg/ml) followed by heart puncture with a syringe rinsed with heparin (5,000 IE/ml). The mice in the blocked group were euthanized at 1 h after injection. Blood and organ samples: lung, liver, spleen, kidneys, tumor, muscle, bone, gastrointestinal tract (with content) and the remaining carcass were collected, weighed and the radioactivity measured as describe above. The whole spectra for each sample were recorded immediately after injection and 24 h later (after complete decay of <sup>68</sup>Ga). The data were corrected for background radiation, gamma spectrometer dead time percentage during each measurement, and decay during measurement. Based on the second measurement, organ uptake values for <sup>111</sup>In were calculated as percent of injected dose per gram of tissue (%ID/g), except for the gastrointestinal tract and the remaining carcass, which were calculated as %ID per whole sample. Thereafter, indium counts were corrected for decay (using a <sup>111</sup>In standard) and subtracted from counts obtained during first measurement (immediately after dissection). The resulted values presented radioactivity of <sup>68</sup>Ga in each organ during the first measurement. These values were used to calculate biodistribution of <sup>68</sup>Ga-labeled tracer.

As a comparator for DOTA-Z<sub>HER2:342min</sub>, an additional biodistribution study on the same animal batch with the same xenograft model was performed using <sup>111</sup>In- and <sup>68</sup>Ga- labeled PEP09239. A group of four mice were injected intravenously (tail vein) with 3.51 µg, 10 kBq (<sup>111</sup>In-PEP09239) and 380 kBq (<sup>68</sup>Ga-PEP09239), in 100 µL PBS per animal and the biodistribution of the radioactivity was measured as described above.

## RESULTS

### Production, Purification and Identification of DOTA-Z<sub>HER2:342min</sub>

Purity of the backbone-cyclized peptide was confirmed by ESI-MS (Molecular formula: C<sub>186</sub>H<sub>291</sub>N<sub>57</sub>O<sub>56</sub>S<sub>2</sub>, Mw expected and detected: 4286 Da). No linear peptide was detected after this step, indicating that all of the linear peptide was converted to the cyclic structure. After cyclization, DOTA-maleimide was coupled to the cysteine residue in position 3 (numbering according to the original 3-helix Z<sub>HER2:342</sub> sequence) (**Figure 1**). Conjugation was confirmed by ESI-MS (Mw expected and detected: 4812 Da).

### Helicity and Thermal Stability of DOTA-Z<sub>HER2:342min</sub>

CD spectroscopy was used to confirm that the cyclic DOTA-Z<sub>HER2:342min</sub> adopted a helical structure. As expected, the spectra showed the characteristics of  $\alpha$ -helical structure with minima at 208 and 220 nm and a maximum between 194 and 196 nm (**Figure 2**). When exposed to heat treatment (20-90 C gradient), DOTA-Z<sub>HER2:342min</sub> lost its helical conformation. No exact transition temperature could be estimated since the conversion was gradual (data not shown). When cooled down to ambient temperature, the protein adopted the same helical structure as prior to heat treatment (**Figure 2**).

### Affinity and Selectivity of DOTA-Z<sub>HER2:342min</sub> towards HER2

Analysis of the binding kinetics showed that DOTA-Z<sub>HER2:342min</sub> has high affinity towards its target receptor with a determined dissociation constant K<sub>D</sub> of 18 nM (**Figure 3**). No

interaction with the negative control was detected, suggesting that DOTA-Z<sub>HER2:342min</sub> is selective for its target (data not shown). The affinity of the 2-helix DOTA-Z<sub>HER2:342min</sub> Affibody variant for binding to HER2 is approximately 10<sup>3</sup> times lower than the affinity of the corresponding, original 3-helix Affibody molecule. This is in line with data reported earlier on other 2-helix versions of HER2-binding 3-helix Affibody molecules [16-18].

### **Radiolabeling of Conjugates with <sup>111</sup>In and <sup>68</sup>Ga**

Radiochemical yields of 98.75 ± 3.4% and 99.7 ± 0.0% were achieved for <sup>111</sup>In-DOTA-Z<sub>HER2:342min</sub> and <sup>111</sup>In-PEP09239 with specific activities of about 0.8 MBq/μg (3.9 GBq/μmol). The labeling yield was lower than standard value (95%), when adding 80 MBq of <sup>68</sup>Ga. It can be due to the higher amount of impurity in the eluted fraction. Decreasing the activity to 40 MBq improved the yield considerably; analytical radiochemical yield was 92.2 ± 1.9% (specific activity about 2 MBq/μg, 9.6 GBq/μmol) and 97.1 ± 0.3% (specific activity about 0.8 MBq/μg, 3.9 GBq/μmol) for <sup>68</sup>Ga-DOTA-Z<sub>HER2:342min</sub> and <sup>68</sup>Ga-PEP09239, respectively. Identity of <sup>68</sup>Ga-DOTA-Z<sub>HER2:342min</sub> was confirmed using SDS-PAGE (**Figure 4**).

The EDTA challenge demonstrated very high labeling stability. The radiochemical purity of <sup>68</sup>Ga-DOTA-Z<sub>HER2:342min</sub> after challenge with 500-fold EDTA excess was 98.3±0.4% and 99.2±0.3%, for EDTA-treated samples and control samples, respectively. The radiochemical purity of <sup>111</sup>In-DOTA-Z<sub>HER2:342min</sub> was 98.3±0.3% and 98.9±0.1%, for EDTA-treated samples and control samples, respectively.

### ***In Vitro* Binding Property Evaluation of Labeled Conjugates**

The kinetics measurements of 2-helix Affibody molecules binding to HER2-expressing SKOV-3 cells *in vitro* using LigandTracer confirmed that antigen-binding capacity was preserved after labeling. The sensorgrams are presented on **Figure 5**. The fact that binding curves approach equilibrium demonstrated saturable character of the binding. Evaluation of data by fitting the binding curves from the affinity titration to a 1:2 interaction model indicates that the binding of radiolabeled conjugates to living HER2-expressing cells is mediated by two binding site populations, one strong and one weaker interaction of approximate 7.31 and 429 nM for  $^{68}\text{Ga}$ -DOTA- $Z_{\text{HER2}:342\text{min}}$  (**Figure 5**). The presence of strong and weak interactions was also found for the three other radioconjugates (**Table 1**). The strong component of the interaction was in low nanomolar to subnanomolar range for all variants. Interestingly, binding of  $^{111}\text{In}$ -labeled 2-helix Affibody molecules was stronger than their  $^{68}\text{Ga}$ -labelled counterparts.

### ***In Vivo* Biodistribution Studies**

Data concerning targeting of HER2-expressing SKOV-3 xenografts in BALB/c *nu/nu* mice using  $^{68}\text{Ga}$ -DOTA- $Z_{\text{HER2}:342\text{min}}$  and  $^{111}\text{In}$ -DOTA- $Z_{\text{HER2}:342\text{min}}$  at 1 h and 2 h post injection are presented in **Figure 6, 7, and 8**. Pre-saturation of HER2 receptors in tumor xenografts using non-labeled  $Z_{\text{HER2}:342}$  Affibody molecule reduced the tumor uptake of both  $^{68}\text{Ga}$ -DOTA- $Z_{\text{HER2}:342\text{min}}$  and  $^{111}\text{In}$ -DOTA- $Z_{\text{HER2}:342\text{min}}$  significantly (**Figure 6**), which confirms the specificity of the radioconjugates' binding to HER2 *in vivo*. Biodistribution studies demonstrated rapid blood clearance of both radioconjugates (**Figure 7**). Radioactivity in the gastrointestinal tract with content was low (less than 2% of injected radioactivity), which suggests that hepatobiliary excretion played only a minor role in the elimination of radiolabeled  $Z_{\text{HER2}:342\text{min}}$ . More apparent was renal excretion with subsequent tubular

reabsorption, as kidney uptake was more than 150% ID/g for both radioconjugates. Although general biodistribution patterns of  $^{111}\text{In-DOTA-Z}_{\text{HER2}:342\text{min}}$  and  $^{68}\text{Ga-DOTA-Z}_{\text{HER2}:342\text{min}}$  were similar, uptake in normal organs differed significantly between radioconjugates. Surprisingly,  $^{68}\text{Ga-DOTA-Z}_{\text{HER2}:342\text{min}}$  uptake in lung ( $23.25 \pm 16.40\%$  and  $12.09 \pm 4.76\%$  at 1 and 2 hours after injection, respectively) was nearly five-fold higher than that of  $^{111}\text{In-DOTA-Z}_{\text{HER2}:342\text{min}}$ . The liver uptake of  $^{111}\text{In-DOTA-Z}_{\text{HER2}:342\text{min}}$  ( $9.78 \pm 0.61\%$  and  $12.02 \pm 1.88\%$ , at 1 and 2 hours after injection, respectively) exceeded significantly ( $p < 0.05$  in a paired t-test) uptake of  $^{68}\text{Ga-DOTA-Z}_{\text{HER2}:342\text{min}}$  ( $8.06 \pm 0.98\%$  and  $10.54 \pm 2.04\%$ ) in both time-points.  $^{68}\text{Ga-DOTA-Z}_{\text{HER2}:342\text{min}}$  displayed slightly higher spleen uptake than  $^{111}\text{In-DOTA-Z}_{\text{HER2}:342\text{min}}$ . Tumor uptake of  $^{111}\text{In-DOTA-Z}_{\text{HER2}:342\text{min}}$  was slightly, 1.2-fold, but significantly ( $p < 0.05$  in paired t-test) higher than uptake of  $^{68}\text{Ga-DOTA-Z}_{\text{HER2}:342\text{min}}$  at both time points. The difference between tumor uptake at 1 and 2 hours after injection was not significant for both conjugates. Tumor-to-blood, and tumor-to-muscle, tumor-to-lung, and tumor-to-bone ratios were significantly higher for  $^{111}\text{In-DOTA-Z}_{\text{HER2}:342\text{min}}$  at 1 and 2 h after injection (**Figure 8**).

$^{111}\text{In-PEP09239}$  and  $^{68}\text{Ga-PEP09239}$  were used as comparators for  $^{111}\text{In-DOTA-Z}_{\text{HER2}:342\text{min}}$  and  $^{68}\text{Ga-DOTA-Z}_{\text{HER2}:342\text{min}}$ . One group of tumor-bearing animals from the same batch was used to study biodistribution of  $^{111}\text{In-PEP09239}$  and  $^{68}\text{Ga-PEP09239}$  at 1 h after injection (**Table 2**). The data for biodistribution of  $^{111}\text{In-PEP09239}$  were in a good agreement with previous studies [18].  $^{111}\text{In-PEP09239}$  and  $^{68}\text{Ga-PEP09239}$  provided approximately four-fold higher radioactivity uptake in tumors. Besides, uptake of  $^{111}\text{In-DOTA-Z}_{\text{HER2}:342\text{min}}$  and  $^{68}\text{Ga-DOTA-Z}_{\text{HER2}:342\text{min}}$  was appreciably higher in lungs, liver and spleen. Tumor-to-blood, tumor-to-liver, and tumor-to-spleen ratios were higher for PEP09239.

## DISCUSSION

Developing of molecular imaging has substantial potential in identifying and characterization of disease-specific biomarkers. Imaging of these biomarkers holds great promise to better define treatment, stratify patients and evaluate therapeutic response [23]. When choosing an appropriate targeting agent for molecular imaging, scaffold proteins with high proteolytic stability, resistance to elevated temperatures, and long-term shelf life as well as fast kinetics are considered as one of the best options [24]. The Affibody scaffold, a 58 amino acid residue domain, has been extensively used as a targeting agent in several studies for therapeutic and diagnostic purposes. The relatively small number of amino acid residues in the scaffold enables synthesis of Affibody molecules by solid phase peptide synthesis (SPPS). Chemical synthesis in turn makes it possible to modify or add specific moieties to the scaffold in a convenient way. Decreasing the size of Affibody molecules might give rise to advantageous properties, such as better solubility, improved tissue penetration, more rapid clearance of non-bound tracer and comparatively low production costs. Previous studies [16-18] have proven that truncated 2-helix Affibody scaffolds display faster *in vivo* kinetics than their 3-helix variants. Although tumor uptake of these 2-helix scaffolds decreased appreciably in comparison with the parental 3-helix variant, tumor-to-organ ratios increased significantly due to elevated clearance of non-bound tracers. The lower tumor uptake of 2-helix variants can be explained by lower affinity and lower bioavailability of the radioconjugates due to the faster blood clearance. Since tumor-to-organ and especially tumor-to-blood ratios are important parameters in image contrast, development of 2-helix scaffolds is an interesting approach to obtaining the high contrast molecular imaging even if the tumor uptake is lower.

The use of NCL for stabilization of the structure of 2-helix Affibody molecules offers a number of potential advantages, such as potentially higher resistance to exopeptidases, possibility to perform labeling in the presence of strong reducing or oxidizing agents, and possibility of site-specific labeling using thiol-directed chemistry. However, Z<sub>HER2:342min</sub> differs appreciably from the previously described variant (MUT-DS, PEP09239). A total of 10 amino acid were deleted or substituted, and Z<sub>HER2:342min</sub> is shorter than PEP09239 (35 aa vs 39 aa). In addition, different chemistry was used for conjugation of the DOTA chelator. Earlier experience with Affibody molecules has suggested that even smaller changes in composition (substitution of one to three amino acids) could cause appreciable differences in biodistribution, such as the level of hepatic uptake [25, 26] or percentage of hepatobiliary excretion [27-29]. Moreover, coupling of different nuclides using the same chelator could cause differences in organ uptake and blood clearance rate of Affibody molecules [21, 29, 30]. This necessitated careful characterization of the new Z<sub>HER2:342min</sub> variant both *in vitro* and *in vivo*.

The engineered 2-helix Affibody Z<sub>HER2:342min</sub> showed a preserved specificity of binding to HER2. The affinity toward its target (18 nM, as measured using Biacore) (**Figure 3**) was substantially decreased in comparison with the parental 3-helix Z<sub>HER2:342</sub> Affibody molecule (22 pM) [4]. However, previous studies have demonstrated that low nanomolar affinity of Affibody molecules is suitable for imaging of abundantly expressed HER2 [4, 15-18,31]. Importantly, the structure of DOTA-Z<sub>HER2:342min</sub> was completely restored after heat treatment (**Figure 2**), which is essential as the labeling using DOTA requires elevated temperatures.

DOTA-Z<sub>HER2:342min</sub> was successfully labeled with <sup>111</sup>In (for imaging using SPECT) and <sup>68</sup>Ga (for imaging using PET) with retained binding capacity. *In vitro* studies with HER2-expressing cells using LigandTracer indicated that interaction of tracers with receptors could

be described by two different binding affinities (**Table 1**): one nanomolar affinity and one substantially lower. It is important to point out that the difference between affinity values measured using Biacore and LigandTracer can be explained by the difference of the methods. Biacore evaluates the binding kinetics using an artificial system with immobilized receptors, while LigandTracer assays are performed on living cells. Previously it has been shown that ligands binding to the HER family receptors on living cells display various kinetics and affinity characteristics [32,33]. Presence of other HER family members as well as activation processes due to the homo- and hetero-dimerization of the receptors [34] might affect the binding kinetics and affinity. The difference in ligand interaction kinetics with the same overexpressed receptor in different cell lines has previously been demonstrated using LigandTracer [35]. Biphasic binding of 3-helix Affibody molecules to living cell lines has been found earlier using LigandTracer [33]. Interestingly, affinity of  $^{111}\text{In}$ -labeled variants was higher than  $^{68}\text{Ga}$ -labeled for both DOTA- $Z_{\text{HER2}:342\text{min}}$  and PEP09239. It has to be noted that  $^{68}\text{Ga}$  and  $^{111}\text{In}$  complexes of DOTA have different geometry [36], which influences structure and affinity of labeled peptides.

*In vivo*, both  $^{68}\text{Ga}$ -DOTA- $Z_{\text{HER2}:342\text{min}}$  and  $^{111}\text{In}$ -DOTA- $Z_{\text{HER2}:342\text{min}}$  were able to specifically target HER2-expressing SKOV-3 xenografts (**Figure 6**). The tumor uptake values ( $2.4 \pm 0.5$  and  $2.9 \pm 0.7\%$  ID/g at 1 h after injection for  $^{68}\text{Ga}$ -DOTA- $Z_{\text{HER2}:342\text{min}}$  and  $^{111}\text{In}$ -DOTA- $Z_{\text{HER2}:342\text{min}}$ , respectively) were in agreement with values for the same model (SKOV-3 xenografts) obtained for 3-helix Affibody molecules with similar affinity. For example, uptake of a monomeric 3-helix Affibody  $^{125}\text{I}$ - $Z_{\text{HER2}:4}$  with  $K_D$  of 50 nM (determined by Biacore) was  $4.1 \pm 1.3\%$  ID/g [4]. The tumor uptakes of dimeric  $^{125}\text{I}$ -His<sub>6</sub>-( $Z_{\text{HER2}:4}$ )<sub>2</sub> and  $^{99\text{m}}\text{Tc}$  (CO)<sub>3</sub>-His<sub>6</sub>-( $Z_{\text{HER2}:4}$ )<sub>2</sub> with  $K_D$  of 3 nM (determined by Biacore) were  $3.2 \pm 0.1$  and  $1.9 \pm 0.5\%$  ID/g at 1 h, were in the same range [31]. Blood clearance of 2-helix DOTA- $Z_{\text{HER2}:342\text{min}}$

was significantly faster than 3-helix monomeric and dimeric Affibody molecules. At 2 h after injection, the tumor-to-blood ratios were  $4.6 \pm 0.7$  and  $6.1 \pm 0.5$  for  $^{68}\text{Ga}$ -DOTA- $Z_{\text{HER2}:342\text{min}}$  and  $^{111}\text{In}$ -DOTA- $Z_{\text{HER2}:342\text{min}}$ , respectively. This is the level the best antibody-based HER2-imaging agents display 2-3 days after injection [37].

The dual label approach permitted to reveal different influence of  $^{111}\text{In}$  and  $^{68}\text{Ga}$  on the biodistribution properties of DOTA- $Z_{\text{HER2}:342\text{min}}$ . The blood clearance rate of  $^{111}\text{In}$ -DOTA- $Z_{\text{HER2}:342\text{min}}$  was higher, which resulted in significantly lower blood concentration 1 h after injection. At 2 h after injection, the uptake of  $^{68}\text{Ga}$ -DOTA- $Z_{\text{HER2}:342\text{min}}$  was significantly higher in lung and spleen, but lower in liver and kidneys in comparison to  $^{111}\text{In}$ -DOTA- $Z_{\text{HER2}:342\text{min}}$  (**Figure 7**). The tumor uptake was slightly, but significantly higher for  $^{111}\text{In}$ -DOTA- $Z_{\text{HER2}:342\text{min}}$ . In general,  $^{111}\text{In}$ -DOTA- $Z_{\text{HER2}:342\text{min}}$  provided higher tumor-to-blood, tumor-to-spleen, tumor-to-muscle, and tumor-to-bone ratios (**Figure 8**). These observations are not unusual. For example, earlier studies have demonstrated substantial (2-9 folds) difference in kidney, liver, lungs and spleen uptake of  $^{111}\text{In}$ - and  $^{68/67}\text{Ga}$ -labeled somatostatin analogues [38, 39]. The authors pointed that Ga and In have different coordination numbers in DOTA complexes, which resulted in different local charge distribution [36] and might be a reason for different biodistribution properties. Probably, this is also reason for difference in biodistribution of  $^{111}\text{In}$ - and  $^{68}\text{Ga}$ -labeled DOTA- $Z_{\text{HER2}:342\text{min}}$ .

Biodistribution of DOTA- $Z_{\text{HER2}:342\text{min}}$  was directly (in the same batch of tumor-bearing mice) compared with biodistribution of PEP09239 labeled with  $^{68}\text{Ga}$  and  $^{111}\text{In}$ . The results obtained for the study of  $^{111}\text{In}$ -PEP09239 were in agreement with previously published data [18]. Both  $^{68}\text{Ga}$ - and  $^{111}\text{In}$ -labeled PEP09239 displayed higher tumor uptake than DOTA- $Z_{\text{HER2}:342\text{min}}$  (**Table 2**), which can be explained by the higher affinities of PEP09239-based tracers (**Table**

1). The major issue is, however, that uptake of DOTA-Z<sub>HER2:342min</sub> is appreciably higher in liver, spleen and lung (**Table 2**). This makes tumor imaging problematic, as liver and lungs are metastatic sites for many malignancies.

Higher uptake in lung, liver and spleen of radiolabeled DOTA-Z<sub>HER2:342min</sub> compared to radiolabeled PEP09239 might be due to different reasons. In principle, uptake in these organs might be specific. However, a numerous studies with parental Z<sub>HER2:343</sub> and its derivatives having the same binding site have demonstrated that uptake in these organs is not saturable, and therefore nonspecific [40-44]. Much lower uptake was also for radiolabeled PEP09239 having the same binding site and higher affinity to HER2. Therefore, the specific accumulation might be excluded. Another possible reason for elevated uptake in liver and spleen might be an insufficient labeling stability and release of <sup>111</sup>In and <sup>68</sup>Ga from the chelator. However, the EDTA challenge (see Results section) have demonstrated negligible release of radionuclides from <sup>111</sup>In-Z<sub>HER2:342min</sub> and <sup>68</sup>Ga -Z<sub>HER2:342min</sub>, which was comparable for the two labeled conjugates within the experimental error of the method.. There was no difference in stability of <sup>68</sup>Ga/<sup>111</sup>In-Z<sub>HER2:342min</sub> and <sup>68</sup>Ga/<sup>111</sup>In-PEP09239 [18] in the EDTA challenge test. It has to be noted that biodistribution studies with the 3-helix variant labeled with <sup>111</sup>In using a maleimido derivative of DOTA showed much lower uptake in liver and spleen (0.9±0.1% ID/g and 0.48±0.0.6% ID/g at 1 h after injection, respectively). Our recent studies with the 3-helix scaffold labeled with <sup>68</sup>Ga using a maleimido DOTA derivative under the same conditions, demonstrated appreciably lower uptake in liver and spleen, 3.2±0.4 % ID/g and 1.8±0.3 % ID/g, respectively at 1 h after injection (Tolmachev, unpublished results). Thus, it is unlikely that <sup>111</sup>In and <sup>68</sup>Ga were released from the chelator. In addition, we have earlier directly compared an <sup>111</sup>In-labeled recombinant 3-helix Affibody molecule conjugated to maleimido DOTA through C-terminal cysteine with a synthetic counterpart

conjugated to DOTA via an amide bond [40]. We have not found any significant difference in liver uptake between these two conjugates. This means that the coupling chemistry between chelator and Affibody molecules does not influence the liver and spleen uptake. Transfer of a maleimido-conjugated chelator from Affibody molecules to albumin or other molecules having free thiols does, most likely, not occur to any noticeable extent during shorter time periods in blood, and does not contribute to elevated off-target uptake. Taken this into account, the high uptake in lungs, liver and spleen may be attributed to the difference in amino acid composition. Elevated uptake of radiopeptides in these organs is usually associated with higher hydrophobicity. Indeed, evaluation using two scales of amino acid hydrophobicity [45, 44] suggests that  $Z_{\text{HER2}:342\text{min}}$  is slightly more hydrophobic than PEP09239. Our previous studies on 3-helix Affibody molecules suggest that such minor difference might be enough to cause noticeable increase of hepatic uptake and/or hepatobiliary excretion [47]. We propose that substitution of non-binding residues (blue residues in **Figure 1**) to other charged or polar amino acids, such as serine, threonine, aspartate or glutamate, to increase the hydrophilicity of the  $Z_{\text{HER2}:342\text{min}}$  scaffold, might improve its biodistribution profile and *in vivo* targeting potential. Other positions that could be substituted include the amino acids introduced to facilitate synthesis and cyclization (green residues in **Figure 1**), such as the two amino acids flanking the intramolecular ligation site. Two glycine residues were chosen to increase the flexibility and aid the cyclization reaction, but one could speculate that any small amino acid might be incorporated at the ligation site without losing cyclization ability or target affinity.

In conclusion, the use of NCL-cyclization enables production of a 2-helix  $Z_{\text{HER2}:342\text{min}}$  Affibody molecule that possesses high refolding capacity, permits site-specific radiolabelling, and has reasonably good affinity to its molecular target. Target specificity is preserved upon

DOTA-mediated labeling with  $^{111}\text{In}$  and  $^{68}\text{Ga}$ , and enabled target-mediated accumulation in tumor xenografts. The presented 2-helix based binder does not perform as well as 3-helix binders with regard to target affinity and displays increased radioactivity uptake in lung, liver and spleen compared to a disulfide-stabilized 2-helix Affibody. However, the 2-helix scaffold has a decreased total amount of amino acid residues, which facilitates production both from a synthesis and economical viewpoint. Further, the backbone cyclization by NCL creates a robust scaffold that eliminates the risk of exoprotease degradation, thiol-disulfide exchange and reduction of the disulfide *in vivo*. The cysteine residue at the ligation point between helices 1 and 2 can be used as a chemo-selective handle for conjugation of chelators and linker for radionuclides. Additional advantageous properties of the smaller 2-helix scaffold include possible higher tissue penetration and a more rapid blood clearance.

#### **ACKNOWLEDGEMENT**

The study was supported by a grant in the SAMBIO program from VINNOVA, from Swedish Cancer Society (Cancerfonden) and Swedish Research Council (Vetenskapsrådet). The authors are grateful to Dr. Lars Abrahmsén, Dr Joachim Feldwisch, and Dr. Caroline Ekblad for helpful discussions during the course of the project.

## REFERENCES

- [1] Nygren PÅ. Alternative binding proteins: affibody binding proteins developed from a small three-helix bundle scaffold. *The FEBS journal* 2008;275:2668-76.
- [2] Löfblom J, Feldwisch J, Tolmachev V, Carlsson J, Ståhl S, and Frejd FY. Affibody molecules: engineered proteins for therapeutic, diagnostic and biotechnological applications. *FEBS letters* 2010;584:2670-80.
- [3] Ahlgren S and Tolmachev V. Radionuclide molecular imaging using Affibody molecules. *Curr Pharm Biotechnol.* 2010;11:581-9.
- [4] Orlova A, Magnusson M, Eriksson TL, Nilsson M, Larsson B, Hoiden-Guthenberg I, et al. Tumor imaging using a picomolar affinity HER2 binding affibody molecule. *Cancer Res* 2006;66:4339-48.
- [5] Tolmachev V, Rosik D, Wållberg H, Sjöberg A, Sandström M, Hansson M, et al. Imaging of EGFR expression in murine xenografts using site-specifically labelled anti-EGFR <sup>111</sup>In-DOTA-Z EGFR:2377 Affibody molecule: aspect of the injected tracer amount. *Eur J Nucl Med Mol Imaging* 2010;37:613-22.
- [6] Kronqvist N, Malm M, Gostring L, Gunneriusson E, Nilsson M, Hoiden Guthenberg I, et al. Combining phage and staphylococcal surface display for generation of ErbB3-specific Affibody molecules. *Protein engineering, design & selection : PEDS* 2011;24:385-96.
- [7] Lindborg M, Cortez E, Hoiden-Guthenberg I, Gunneriusson E, von Hage E, Syud F, et al. Engineered high-affinity affibody molecules targeting platelet-derived growth factor receptor beta in vivo. *J Mol Biol.* 2011;407:298-315.
- [8] Tolmachev V, Malmberg J, Hofstrom C, Abrahmsén L, Bergman T, Sjöberg A, et al. Imaging of insulinlike growth factor type 1 receptor in prostate cancer xenografts using the affibody molecule <sup>111</sup>In-DOTA-ZIGF1R:4551. *J Nucl Med;* 2012;53:90-7.

- [9] Orlova A, Wällberg H, Stone-Elander S, and Tolmachev V. On the selection of a tracer for PET imaging of HER2-expressing tumors: direct comparison of a  $^{124}\text{I}$ -labeled affibody molecule and trastuzumab in a murine xenograft model. *J Nucl Med*; 2009;50:417-25.
- [10] Malmberg J, Sandström M, Wester K, Tolmachev V, and Orlova A. Comparative biodistribution of imaging agents for in vivo molecular profiling of disseminated prostate cancer in mice bearing prostate cancer xenografts: focus on  $^{111}\text{In}$ - and  $^{125}\text{I}$ -labeled anti-HER2 humanized monoclonal trastuzumab and ABY-025 affibody. *Nucl Med Biol*; 2011;38:1093-102.
- [11] Baum RP, Prasad V, Muller D, Schuchardt C, Orlova A, Wennborg A, et al. Molecular imaging of HER2-expressing malignant tumors in breast cancer patients using synthetic  $^{111}\text{In}$ - or  $^{68}\text{Ga}$ -labeled affibody molecules. *J Nucl Med*; 2010;51:892-7.
- [12] Sandberg D, Wennborg A, Feldwisch J, Tolmachev V, Carlsson J, Garske U, et al. First clinical observations of HER2 specific [ $^{111}\text{In}$ ]ABY-025 metastatic detection capability in females with metastatic breast cancer. *J Nucl Med*; 2012;220 Abstract.
- [13] Starovasnik MA, Braisted AC, and Wells JA. Structural mimicry of a native protein by a minimized binding domain. *Proc Natl Acad Sci U S A*. 1997;94:10080-5.
- [14] Webster JM, Zhang R, Gambhir SS, Cheng Z, and Syud FA. Engineered two-helix small proteins for molecular recognition. *ChemBioChem* 2009;10:1293-6.
- [15] Tolmachev V, Tran TA, Rosik D, Sjöberg A, Abrahmsén L, and Orlova A. Tumor targeting using affibody molecules: interplay of affinity, target expression level, and binding site composition. *J Nucl Med*; 2012;53:953-60.
- [16] Ren G, Zhang R, Liu Z, Webster JM, Miao Z, Gambhir SS, et al. A 2-helix small protein labeled with  $^{68}\text{Ga}$  for PET imaging of HER2 expression. *J Nucl Med*; 2009;50:1492-9.
- [17] Ren G, Webster JM, Liu Z, Zhang R, Miao Z, Liu H, et al. In vivo targeting of HER2-positive tumor using 2-helix affibody molecules. *Amino acids* 2012;43:405-13.

- [18] Rosik D, Orlova A, Malmberg J, Altai M, Varasteh Z, Sandström M, et al. Direct comparison of  $^{111}\text{In}$ -labelled two-helix and three-helix Affibody molecules for in vivo molecular imaging. *Eur J Nucl Med Mol Imaging* 2012;39:693-702.
- [19] Järver P, Mikaelsson C, and Karlström AE. Chemical synthesis and evaluation of a backbone-cyclized minimized 2-helix Z-domain. *J Pept Sci.* 2011;17:463-9.
- [20] Braisted AC and Wells JA. Minimizing a binding domain from protein A. *Proc Natl Acad Sci U S A.* 1996;93:5688-92.
- [21] Tolmachev V, Velikyan I, Sandström M, and Orlova A. A HER2-binding Affibody molecule labelled with  $^{68}\text{Ga}$  for PET imaging: direct in vivo comparison with the  $^{111}\text{In}$ -labelled analogue. *Eur J Nucl Med Mol Imaging* 2010;37:1356-67.
- [22] Björke H and Andersson K. Automated, high-resolution cellular retention and uptake studies in vitro. *Appl Radiat Isot.* 2006;64:901-5.
- [23] Weissleder R. Molecular imaging in cancer. *Science* 2006;312:1168-71.
- [24] Nygren PÅ and Skerra A. Binding proteins from alternative scaffolds. *J Immunol Methods* 2004;290:3-28.
- [25] Tran TA, Ekblad T, Orlova A, Sandström M, Feldwisch J, Wennborg A, et al. Effects of lysine-containing mercaptoacetyl-based chelators on the biodistribution of  $^{99\text{m}}\text{Tc}$ -labeled anti-HER2 Affibody molecules. *Bioconj Chem*; 2008;19:2568-76.
- [26] Tolmachev V, Hofstrom C, Malmberg J, Ahlgren S, Hosseinimehr SJ, Sandstrom M, et al. HEHEHE-tagged affibody molecule may be purified by IMAC, is conveniently labeled with  $^{99\text{m}}\text{Tc}(\text{CO})_3(+)$ , and shows improved biodistribution with reduced hepatic radioactivity accumulation. *Bioconj Chem*; 2010;21:2013-22.
- [27] Engfeldt T, Tran T, Orlova A, Widström C, Feldwisch J, Abrahmsen L, et al.  $^{99\text{m}}\text{Tc}$ -chelator engineering to improve tumour targeting properties of a HER2-specific Affibody molecule. *Eur J Nucl Med Mol Imaging* 2007;34:1843-53.

- [28] Tran T, Engfeldt T, Orlova A, Sandström M, Feldwisch J, Abrahmsén L, et al.  $^{99m}\text{Tc}$ -maEEE-Z(HER2:342), an Affibody molecule-based tracer for the detection of HER2 expression in malignant tumors. *Bioconjug Chem*; 2007;18:1956-64.
- [29] Orlova A, Tran TA, Ekblad T, Karlström AE, and Tolmachev V.  $^{186}\text{Re}$ -maSGS-Z (HER2:342), a potential Affibody conjugate for systemic therapy of HER2-expressing tumours. *Eur J Nucl Med Mol Imaging* 2010;37:260-9.
- [30] Wällberg H, Ahlgren S, Widström C, and Orlova A. Evaluation of the radiocobalt-labeled [MMA-DOTA-Cys<sup>61</sup>]-Z<sub>HER2:2395</sub>(-Cys) affibody molecule for targeting of HER2-expressing tumors. *Mol Imaging Biol.* 2010;12:54-62.
- [31] Orlova A, Nilsson FY, Wikman M, Widström C, Ståhl S, Carlsson J, et al. Comparative in vivo evaluation of technetium and iodine labels on an anti-HER2 affibody for single-photon imaging of HER2 expression in tumors. *J Nucl Med*; 2006;47:512-9..
- [32] Özcan F, Klein P, Lemmon MA, Lax I, and Schlessinger J. On the nature of low- and high-affinity EGF receptors on living cells. *Proc Natl Acad Sci U S A.* 2006;103:5735-40.
- [33] Barta P, Malmberg J, Melicharova L, Strandgård J, Orlova A, Tolmachev V, et al. Protein interactions with HER-family receptors can have different characteristics depending on the hosting cell line. *Int J Oncol.* 2012;40:1677-82.
- [34] Tao RH and Maruyama IN. All EGF(ErbB) receptors have preformed homo- and heterodimeric structures in living cells. *J Cell Sci* 2008;121:3207-17.
- [35] Björkelund H, Gedda L, and Andersson K. Comparing the epidermal growth factor interaction with four different cell lines: intriguing effects imply strong dependency of cellular context. *PloS One* 2011;6:e16536.
- [36] Heppeler A, Froidevaux S, Mäcke H, Jermann E, Behe M, Powell P, et al. Radiometal-labelled macrocyclic chelator-derivatisedsomatostatin analogue with superb tumor-targeting

properties and potential for receptor-mediated internal radiotherapy. *Chem Eur J* 1999;5:1974-81.

[37] Tolmachev V. Imaging of HER-2 overexpression in tumors for guiding therapy. *Curr Pharm Des.* 2008;14:2999-3019.

[38] Froidevaux S, Eberle AN, Christe M, Sumanovski L, Heppeler A, Schmitt JS, Eisenwiener K, Beglinger C, Mäcke HR. Neuroendocrine tumor targeting: study of novel gallium-labeled somatostatin radiopeptides in a rat pancreatic tumor model. *Int J Cancer.* 2002;98:930-7.

[39] Antunes P, Ginj M, Zhang H, Waser B, Baum RP, Reubi JC, Maecke H. Are radiogallium-labelled DOTA-conjugated somatostatin analogues superior to those labelled with other radiometals? *Eur J Nucl Med Mol Imaging.* 2007;34:982-93.

[40] Ahlgren S, Orlova A, Rosik D, Sandström M, Sjöberg A, Baastrup B, Widmark O, Fant G, Feldwisch J, Tolmachev V. Evaluation of Maleimide Derivative of DOTA for Site-Specific Labeling of Recombinant Affibody Molecules. *Bioconjug Chem,* 2008; 19:235-243.

[41] Tolmachev V, Mume E, Sjöberg S, Frejd FY, Orlova A. Influence of valency and labelling chemistry on in vivo targeting using radioiodinated HER2-binding *Eur J Nucl Med Molecular Imaging,* 2009;36:692-701.

[42] Tolmachev V, Altai M, Sandström M, Perols A, Ericsson Karlström A, Boschetti F, Orlova A. Evaluation of a maleimido derivative of NOTA for site-specific labeling of affibody molecules. *Bioconjug Chem,* 2011;22:894-902.

[43] Altai M, Perols A, Eriksson Karlström A, Sandström M, Boschetti F, Orlova A, Tolmachev V. Preclinical evaluation of anti-HER2 Affibody molecules site-specifically labeled with <sup>111</sup>In using a maleimido derivative of NODAGA. *Nucl Med Biol* 2012; 39: 518-529

[44] Malmberg J, Perols A, Varasteh Z, Altai M, Sandström M, Garske U, Tolmachev V, Orlova A, Eriksson Karlström A. Comparative evaluation of synthetic anti-HER2 Affibody molecules site-specifically labelled with (<sup>111</sup>)In using N-terminal DOTA, NOTA and NODAGA chelators in mice bearing prostate cancer xenografts.. *Eur J Nucl Med Molecul Imaging*, 2012;39:481-92.

[45] Hopp TP and Woods KR. Prediction of protein antigenic determinants from amino acid sequences. *Proc Natl Acad Sci U S A*. 1981;78:3824-8.

[46] Kyte J and Doolittle RF. A simple method for displaying the hydropathic character of a protein. *J Mol Biol*. 1982;157:105-32.

[47] Hosseinimehr SJ, Tolmachev V, and Orlova A. Liver uptake of radiolabeled targeting proteins and peptides: considerations for targeting peptide conjugate design. *Drug Discov Today*, 2012;17:1224-32.

**Table 1.** Dissociation constants at equilibrium ( $K_D$ ) for binding of radiolabeled 2-helix Affibody molecules to HER2-expressing SKOV-3 cells (measured using LigandTracer).

	<sup>68</sup> Ga-DOTA- $Z_{HER2:342min}$	<sup>111</sup> In-DOTA- $Z_{HER2:342min}$	<sup>68</sup> Ga-PEP09239	<sup>111</sup> In-PEP09239
$K_{D1}(nM)$	7.31	1.1	0.93	0.32
$K_{D2}(nM)$	429	107	15.2	64.1

**Table 2.** Direct comparison of biodistribution of  $^{111}\text{In}$ -DOTA- $Z_{\text{HER2}:342\text{min}}$ ,  $^{111}\text{In}$ -DOTA-PEP09239,  $^{68}\text{Ga}$ -DOTA- $Z_{\text{HER2}:342\text{min}}$ , and  $^{68}\text{Ga}$ -DOTA-PEP09239 in BALB/C nu/nu mice bearing SKOV3 xenografts at 1 h after injection. The concentration of radioactivity is expressed as % ID/g, and presented as an average value from 4 animals  $\pm$  standard deviation.

	$^{68}\text{Ga}$ -DOTA- $Z_{\text{HER2}:342\text{min}}$	$^{68}\text{Ga}$ -DOTA-PEP09239	$^{111}\text{In}$ -DOTA- $Z_{\text{HER2}:342\text{min}}$	$^{111}\text{In}$ -DOTA-PEP09239
blood	0.75 $\pm$ 0.05 <sup>c</sup>	0.59 $\pm$ 0.20 <sup>d</sup>	0.63 $\pm$ 0.05	0.5 $\pm$ 0.2
lung	23 $\pm$ 16 <sup>a</sup>	1.0 $\pm$ 0.2 <sup>d</sup>	4.9 $\pm$ 3.2 <sup>b</sup>	0.7 $\pm$ 0.2
liver	8.1 $\pm$ 1.0 <sup>a, c</sup>	2.4 $\pm$ 0.6 <sup>d</sup>	9.8 $\pm$ 0.6 <sup>b</sup>	1.8 $\pm$ 0.4
spleen	2.5 $\pm$ 0.5 <sup>a</sup>	0.9 $\pm$ 0.4	2.1 $\pm$ 0.4 <sup>b</sup>	0.6 $\pm$ 0.2
kidney	158 $\pm$ 13 <sup>a, c</sup>	280 $\pm$ 39	179 $\pm$ 14 <sup>b</sup>	289 $\pm$ 44
tumor	2.4 $\pm$ 0.5 <sup>a, c</sup>	10.0 $\pm$ 3.2 <sup>d</sup>	2.9 $\pm$ 0.7 <sup>b</sup>	12 $\pm$ 4
muscle	0.18 $\pm$ 0.05	0.16 $\pm$ 0.02	0.17 $\pm$ 0.05	0.15 $\pm$ 0.04
bone	0.45 $\pm$ 0.07 <sup>a</sup>	0.29 $\pm$ 0.04 <sup>d</sup>	0.38 $\pm$ 0.04 <sup>b</sup>	0.20 $\pm$ 0.04
GI tract*	1.1 $\pm$ 0.1	1.6 $\pm$ 0.8	1.3 $\pm$ 0.1	1.7 $\pm$ 0.9

<sup>a</sup> significant difference ( $p < 0.05$  in unpaired test) between  $^{68}\text{Ga}$ -DOTA- $Z_{\text{HER2}:342\text{min}}$  and  $^{68}\text{Ga}$ -DOTA-PEP09239;

<sup>b</sup> significant difference ( $p < 0.05$  in unpaired test) between  $^{111}\text{In}$ -DOTA- $Z_{\text{HER2}:342\text{min}}$  and  $^{111}\text{In}$ -DOTA-PEP09239;

<sup>c</sup> significant difference ( $p < 0.05$  in paired test) between  $^{68}\text{Ga}$ -DOTA- $Z_{\text{HER2}:342\text{min}}$  and  $^{111}\text{In}$ -DOTA- $Z_{\text{HER2}:342\text{min}}$ ;

<sup>d</sup> significant difference ( $p < 0.05$  in paired test) between  $^{68}\text{Ga}$ -DOTA-PEP09239 and  $^{111}\text{In}$ -DOTA-PEP09239;

## Figures captions

**Figure 1.** Schematic drawing of the  $Z_{\text{HER2}:342\text{min}}$  scaffold prior to cyclization. A) Residues conferring HER2-binding specificity in red. B) Residues substituted to increase the solubility in blue. C) The substituted residues compared to the parental Z-domain. Binding residues are colored red, and substitutions to increase solubility are blue. Green marks residues that were introduced to facilitate synthesis and enable subsequent cyclization. Folded in C is the unmodified 3-helix Z-domain. D) Sequence of  $Z_{\text{HER2}:342\text{min}}$ . Coloring is according to description above, and \* indicates DOTA-conjugation site. Amino acid numbering is according to the original 3-helix scaffold.

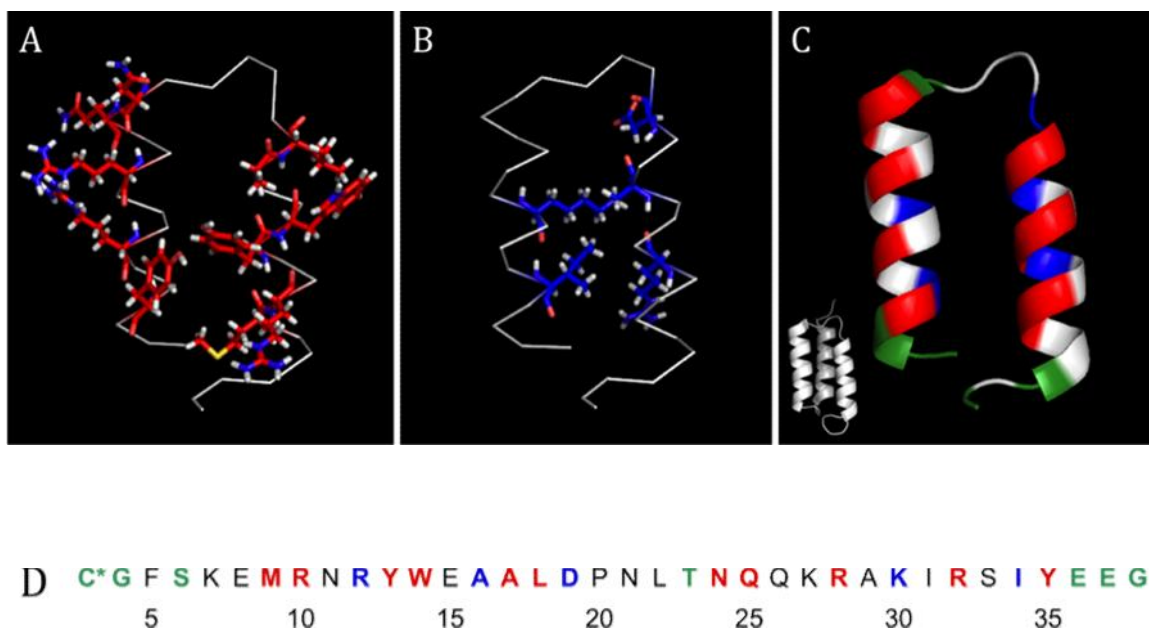


**Figure 2.** CD spectra of DOTA-Z<sub>HER2:342min</sub> before and after exposure to a heat gradient (20-90°C). The protein adopts the same helical structure after the heat treatment. The spectra represent an average of three assembled scans.

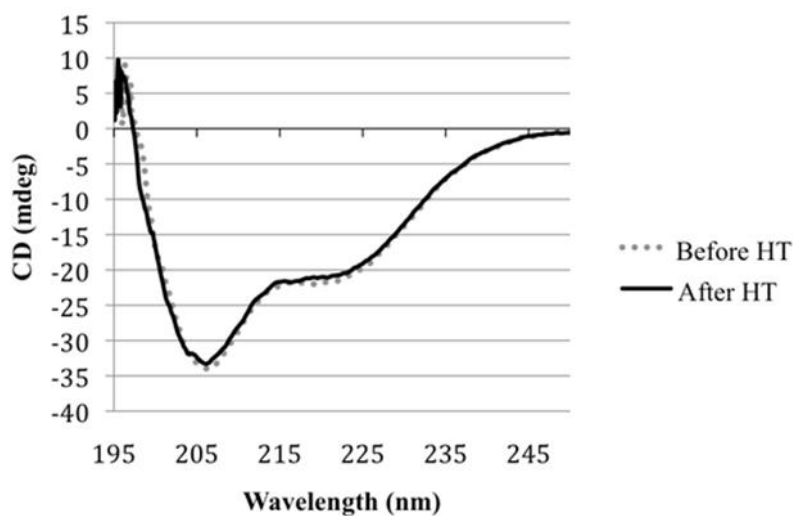


**Figure 3.** Biacore sensorgrams of the interaction of DOTA-Z<sub>HER2:342min</sub> with immobilized HER2. Concentrations of DOTA-Z<sub>HER2:342min</sub> were 2.1-67 nM. The dissociation constant  $K_D$  was estimated to 18 nM.

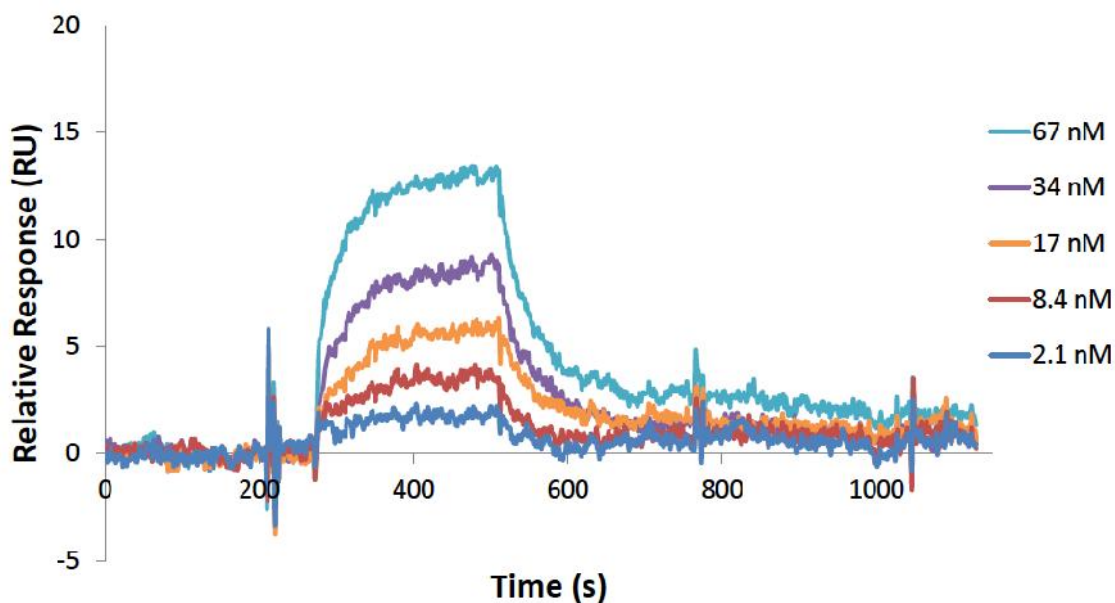


**Figure 4.** Representative SDS-PAGE analysis for identity of  $^{68}\text{Ga}$ -labeled 2-helix scaffold DOTA- $Z_{\text{HER2}:342\text{min}}$  (1), free  $^{68}\text{Ga}$  citrate (2) was used as a marker for low-molecular-weight compounds. The signal was measured as a digital light unit (DLU) in proportion to radioactivity in a given point of a lane in the SDS-PAGE gel.

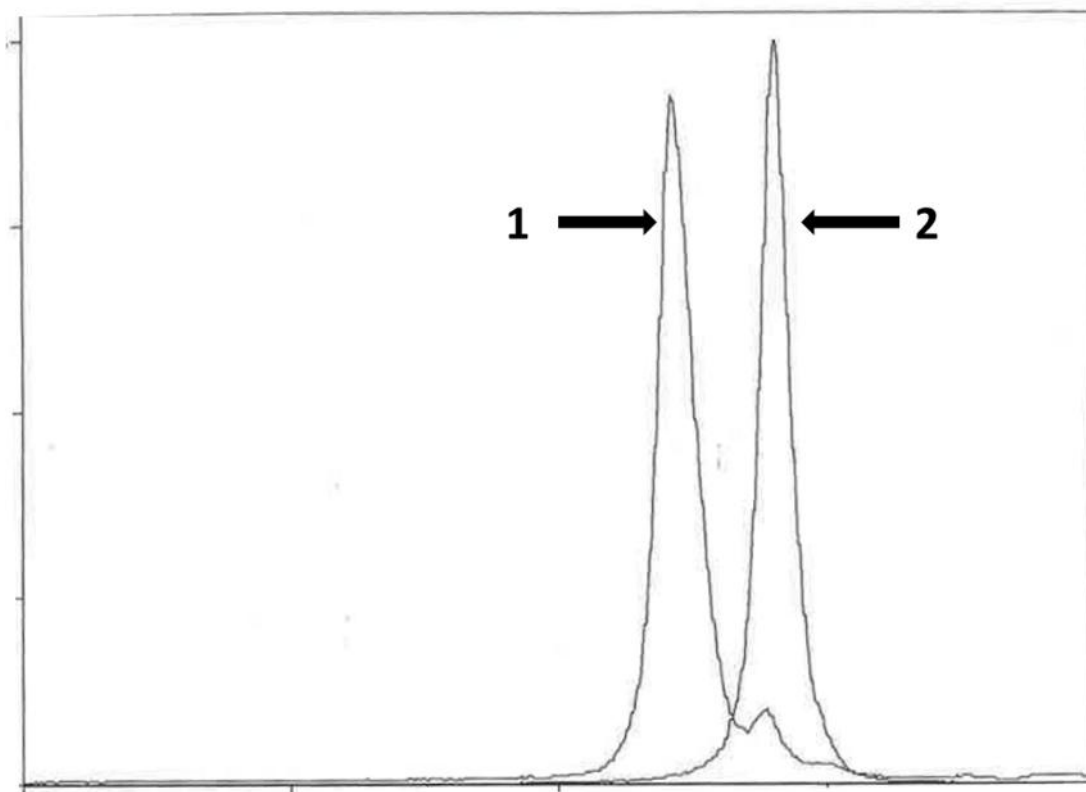


**Figure 5.** LigandTracer sensorgram of interaction of  $^{68}\text{Ga}$ -DOTA- $Z_{\text{HER2}:342\text{min}}$  and  $^{111}\text{In}$ -DOTA- $Z_{\text{HER2}:342\text{min}}$  with HER2-expressing SKOV-3 cells. Concentrations of  $^{68}\text{Ga}$ -DOTA- $Z_{\text{HER2}:342\text{min}}$  were 30 and 100 nM. The dissociation constant  $K_D$  was estimated to 18 nM by Biacore (Figure 3). Fitting binding LigandTracer curves to 1:2 interaction models suggests presence of two interactions, one stronger (7.3 nM) and one weaker (429 nM). The same measurement performed with  $^{111}\text{In}$ -DOTA- $Z_{\text{HER2}:342\text{min}}$  also suggests presence of two interactions, one stronger (1.1 nM) and one weaker (107 nM). The  $^{68}\text{Ga}$ -DOTA- $Z_{\text{HER2}:342\text{min}}$  sensorgram is shifted 100 signal units in the Y-direction to enhance visibility.

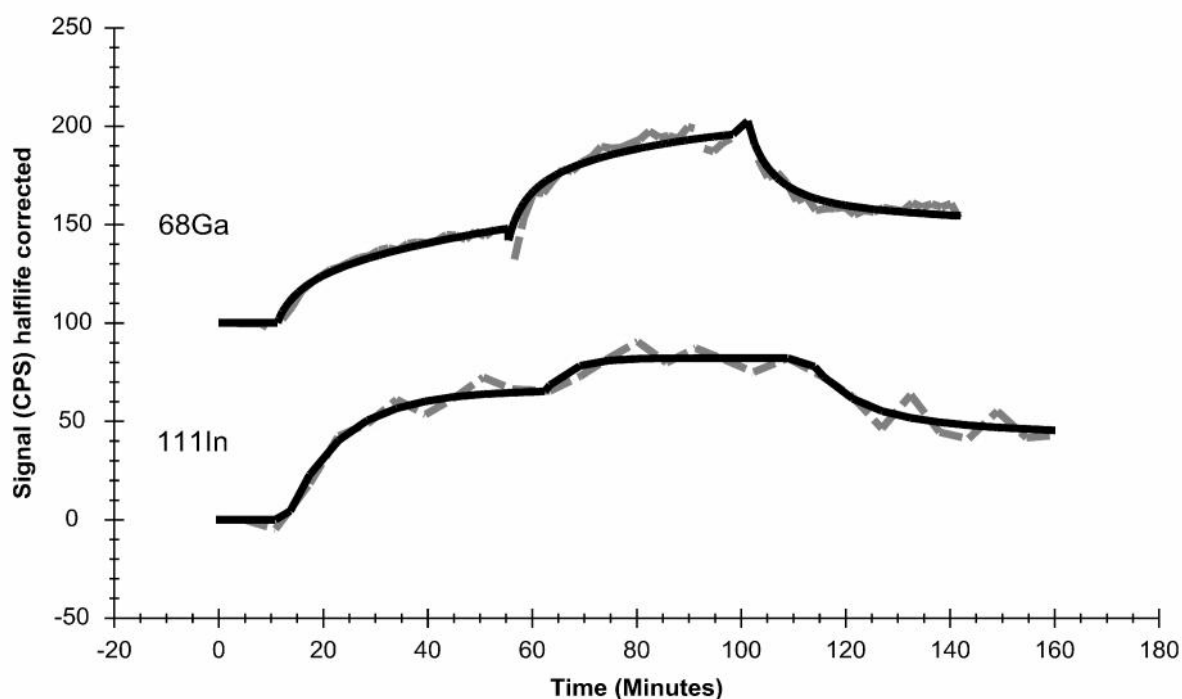


**Figure 6.** In vivo targeting specificity of SKOV-3 xenografts with  $^{68}\text{Ga}$ -DOTA- $Z_{\text{HER2}:342\text{min}}$  (left panel) and  $^{111}\text{In}$ -DOTA- $Z_{\text{HER2}:342\text{min}}$  (right panel), 1 h p.i. The blocked group was subcutaneously pre-injected with an excess amount of non-labeled  $Z_{\text{HER2}:342}$ . Results are presented as percentage of injected dose per gram of tissue (% ID/g). Statistical significance in the tumor uptake between the groups, according to Student's t-test gave  $p < 0.05$ .

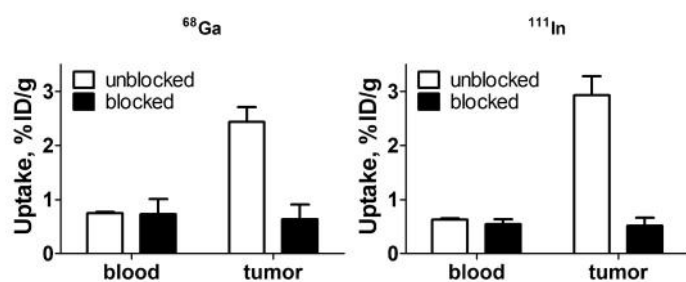


**Figure 7.** Comparative biodistribution of  $^{111}\text{In}$ -DOTA- $Z_{\text{HER2}:342\text{min}}$  and  $^{68}\text{Ga}$ -DOTA- $Z_{\text{HER2}:342\text{min}}$  in BALB/C *nu/nu* mice bearing SKOV-3 xenografts at 1 and 2 h p.i. The concentration of radioactivity is expressed as % ID/g, and presented as an average value from 4 animals  $\pm$  standard deviation. Asterisk (\*) indicate significant difference between  $^{111}\text{In}$  and  $^{68}\text{Ga}$ -labeled conjugates ( $p < 0.05$  in paired Student's t-test).

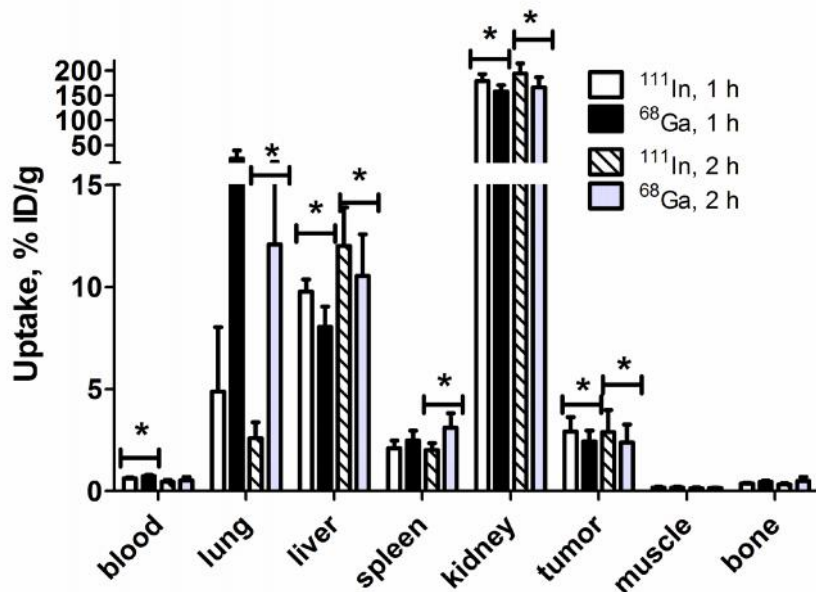


**Figure 8.** Comparison of tumor-to-organ ratios for  $^{111}\text{In}$ -DOTA- $Z_{\text{HER2}:342\text{min}}$  and  $^{68}\text{Ga}$ -DOTA- $Z_{\text{HER2}:342\text{min}}$  in BALB/C *nu/nu* mice bearing SKOV-3 xenografts at 1 and 2 h after injection. Asterisk (\*) indicate significant difference between  $^{111}\text{In}$  and  $^{68}\text{Ga}$ -labeled conjugates ( $p < 0.05$  in paired Student's t-test).

